Calibration and Stereo Tracking of a Laparoscopic Ultrasound Transducer for Augmented Reality in Surgery

Philip Edgcumbe[1], Christopher Nguan[3], and Robert Rohling[1,2]

[1] Department of Electrical and Computer Engineering,
University of British Columbia, Vancouver, BC, Canada
{edgcumbe,rohling}@ece.ubc.ca
[2] Department of Mechanical Engineering,
University of British Columbia, Vancouver, BC, Canada
[3] Department of Urologic Sciences,
University of British Columbia, Vancouver, BC, Canada
chris.nguan@urology.com

Abstract. Laparoscopic ultrasound is a useful adjunct for guidance in minimally invasive surgery. Tracking the location of the ultrasound transducer relative to the laparoscope would enable an augmented reality overlay of subsurface anatomical features on the surgeon's field of view. The accuracy of tracking is a critical aspect for such augmented reality guidance. We propose stereo tracking of visible markers on a new "pick-up" laparoscopic ultrasound transducer and a direct transformation of the ultrasound image into the coordinates of a stereo laparoscope. We also suggest that ultrasound calibration be performed using a separate stereo camera system with a wide baseline. Such calibration is shown to improve point reconstruction accuracy from 3.1 mm to 1.3 mm.

Keywords: Ultrasound, Augmented Reality, Robotic Surgery.

1 Introduction

Minimally invasive surgery (MIS) offers significant advantages compared to open surgery. For example, incisions are smaller, there is less post-operative pain, and a shorter post-operative recovery. However, MIS procedures have disadvantages including: limited view of the surgical field, and reduction of surgical dexterity. Two technologies hold promise to help overcome these disadvantages. These are stereo laparoscopes which improve a surgeon's depth perception and laparoscopic ultrasound (LUS) which improve visualization of subsurface anatomical features. Industry has recognized the demand for stereo laparoscopes as represented firstly, by the inclusion of a stereo laparoscope with the da Vinci Surgical System (Intuitive Surgical, Sunnyvale, CA, UBC), [7] and secondly, by the development of stereo laparoscopes for non-robotic MIS such as the Viking 3DHD Vision System (Viking Systems, Westborough, MA, USA) and the Endoeye Flex 3D (Olympus, Shinjuku, Tokyo, Japan). There is growing interest in the use of

C.A. Linte et al. (Eds.): MIAR/AE-CAI 2013, LNCS 8090, pp. 258–267, 2013.

stereo laparoscopy for standard laparoscopy and for tracking tools and instruments as part of an augmented reality system [8].

LUS improves surgical safety by allowing surgeons to visualize important anatomy beneath the organ surface. 82% of surgeons practicing endoscopy expect an increase in the use of LUS in the next 5-years [17]. To improve the accessibility and ease of interpretation of LUS, several research groups have developed augmented reality LUS systems by tracking the position of a LUS transducer. Offline ultrasound calibration must be performed to determine the transformation from the ultrasound image coordinate system to the LUS transducer marker coordinate system. During ultrasound calibration and during surgery, the accuracy of the tracking of the LUS transducer determines the overall accuracy of the augmented reality LUS system. Tracking of the LUS transducer has been achieved by robotic kinematics [13], optical tracking [9,12], electromagnetic tracking [3], and a combination of optical tracking and electromagnetic tracking [4]. An external base coordinate system, which must be used for tracking with robot kinematics, electromagnetic tracking and external optical tracking, makes tracking susceptible to error amplification due to the lever-arm effect. Maximizing the calibration accuracy is critical to these augmented reality systems.

One of our previous contributions to the field of robotic LUS was the development of a small "pick-up" LUS transducer that can be picked-up by the da Vinci robot and controlled by the surgeon at the da Vinci console [15]. BK Medical (Herlev, Denmark) sells a similar product called the ProART. In this paper we propose an augmented reality LUS system using the new pick-up LUS transducer [15] and stereo laparoscopy. Pratt et al. developed a similar augmented reality LUS system for mono laparoscopy and a pick-up LUS transducer [12]. They used the laparoscope to track the LUS transducer and eliminated the need for an external base coordinate system. This visual tracking of the LUS transducer offers the potential of higher accuracy due to a reduced lever-arm effect and a direct transformation from the ultrasound image to the camera via visible markers on the LUS transducer [12]. Our proposed augmented reality LUS system also uses visual tracking and eliminates the external base coordinate system. Furthermore, we address the problem that stereo laparoscopes have a narrow baseline (camera spacing of about 5 mm) which results in narrow triangulation and poor accuracy of stereo laparoscope augmented reality systems [18].

Our primary innovation is to separate ultrasound calibration and LUS transducer tracking. We use a 75 mm baseline stereo camera for ultrasound calibration and a stereo laparoscope for LUS tracking. For both ultrasound calibration and LUS tracking we use the same LUS optical fiducials and the same tracking method. This approach should reduce the ultrasound calibration error. We measure accuracy by using the tracked LUS to estimate the location of a pinhead of known location in the camera coordinate system. To our knowledge, Leven et al. [9] proposed, but did not report, results for direct visual tracking of a LUS with a stereo laparoscope, so this is the first such report. A second aspect of this project is to characterize the accuracy of an augmented reality LUS system as a function of a changing camera focal length. We do this to understand the

consequences of a surgeon changing the focal length of the stereo laparoscope during surgery to optimize the view of the surgical field [16].

The objective and novelty of this paper is to show how the size of camera baseline during ultrasound calibration affects the error of an augmented reality LUS system.

2 Methods

This section describes the apparatus that was used, the calibration and tracking methods, and the experiments. We compared the combination of a wide baseline calibration and narrow baseline tracking (our proposal) to a combination of narrow baseline calibration and narrow baseline tracking (the standard approach of using the same sensor for calibration and tracking). Accuracy and precision of the two proposed augmented reality LUS systems are reported. Henceforth, the stereo laparoscope will be referred to as a narrow baseline camera.

2.1 Apparatus, Calibration and Tracking

We used a SonixTOUCH ultrasound machine (Ultrasonix Medical Corporation, Richmond, BC, Canada) with a 10MHz LUS transducer (28 mm linear array) [15]. The LUS transducer is designed to take advantage of the dexterity of the da Vinci tools. It can be picked up with the da Vinci Pro-Grasp tool and be moved in all 6 DOF. Furthermore, the surgeon at the da Vinci console controls the movement of the LUS transducer which allows the surgeon's natural hand-eye coordination to aid interpretation of the 3D anatomy from a set of 2D cross-sectional images. All ultrasound images were taken at an ultrasound image depth of 20 mm. All camera images (stereo camera calibration, ultrasound calibration and validation experiments) were taken simultaneously with the two camera systems allowing for a more controlled comparison of the accuracies of the respective camera combinations. The narrow baseline camera is a wide angle NTSC da Vinci stereo laparoscope from the da Vinci Surgical System (Standard). It has a narrow baseline of 5 mm and a resolution of 720 $\times$ 486 pixels. The wide baseline camera system has a baseline of 75 mm and consists of two Flea2 cameras (Point Grey Research, Richmond, Canada) with a resolution of 1280 $\times$ 960 pixels. It has previously been observed that a similar difference in camera resolution did not have a significant effect on camera calibration results [12], so the important difference is the baseline. The calculation of the intrinsic and extrinsic camera parameters and lens distortion coefficients was done with the Caltech Camera Calibration toolbox [2] using about 20 images of unique poses of a 8 $\times$ 10 checkerboard with 5 mm squares.

To define the LUS transducer marker coordinate system we used a similar approach to Pratt et al. [12] in which a small checkerboard is mounted onto the LUS. We placed a 6 $\times$ 2 and a 7 $\times$ 2 checkerboard with 3.175 mm squares on the two flat (9 mm $\times$ 27 mm) surfaces on each side of the LUS transducer [Figure 1]. Our checkerboard is made of surgical identification tape (KeySurgical Inc.,

Eden Prairie, MN, USA) which is approved for internal human use, repeated sterilization cycles and designed to be semi-permanently attached to surgical instruments. Using a camera to track an ultrasound transducer for construction of 3D ultrasound images has been done previously [1].

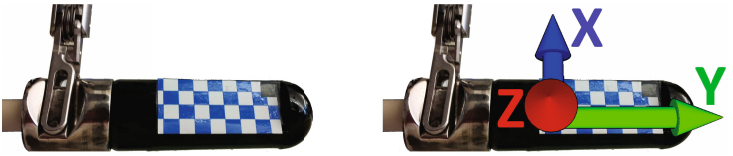

Fig. 1. Left: Picture showing the da Vinci Pro-Grasp tool holding the "pick-up" LUS transducer which has checkerboard markers on it. Right: Same picture as left with addition of 3D coordinate system overlay showing the axes of the LUS transducer marker coordinate system (T). The z axis and the normal of the ultrasound imaging plane are almost parallel.

We used the triple N-wire ultrasound calibration technique [10]. The triple N-wire phantom was precisely manufactured with the Objet30 desktop 3D printer (Objet Inc., Billerica, MA, USA) which has 28 micrometer precision. For defining the location of the N-wires in the coordinate system of the phantom we used an Optotrak Certus optical tracker (Northern Digital Inc, Waterloo, Ontario, Canada) to track four NDI markers on our phantom and an NDI tracked stylus that was used to select the 18 N-wire holes. An Optotrak is not strictly required for this step; we could have used the known geometry of our CAD model to calculate the same geometric relationships. The phantom bath was filled with distilled water and 9% by volume glycerol [11] to achieve a sound speed of 1540 m/s.

For ultrasound calibration and tracking experiments the LUS transducer was placed at a distance of 100 mm from the narrow baseline camera and 150 mm from the wide baseline camera. Figure 2 includes a picture of the experimental setup (left) and a diagram of the four coordinate systems. The coordinate systems are: #1) Ultrasound image coordinate system (I), #2) LUS transducer marker coordinate system (T), #3) Camera coordinate system (C) and #4) Phantom coordinate system (Ph). The camera coordinate system (C) represents either the coordinate system of the wide baseline or narrow baseline camera.

Equation (1) shows the transformation from the ultrasound image coordinate system (x,y with units of mm) to the camera coordinate system (a,b,c with units of mm). The ultrasound calibration matrix - the fixed 6DOF transformation from the ultrasound image to LUS transducer marker coordinate system ($^{T}T_{I}$) - is the part of that equation that is determined offline prior to LUS imaging during surgery. The transformation from the LUS transducer marker coordinate system to the camera coordinate system ($^{C}T_{T}$) is solved by using a corresponding point algorithm between the known location of the 21 saddle points on the transducer checkerboard in the transducer coordinate system and the camera coordinates of

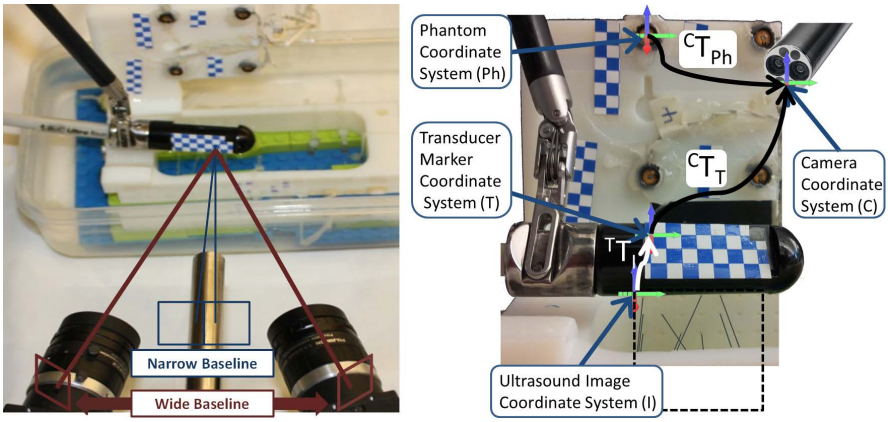

Fig. 2. Two pictures of the experimental setup. Left: The wide baseline and narrow baseline (stereo laparoscope) cameras are in the foreground and the pick-up LUS transducer and triple N-wire phantom are in the background. Right: The LUS transducer, held by the da Vinci Pro-Grasp tool, is directly above the N-wires. The phantom optical fiducials are in the background. The four experimental coordinate systems (I, T, C and Ph) and the transformations between them ($^{C}T_{T}$, $^{T}T_{I}$, $^{C}T_{Ph}$) are shown.

those same saddle points as determined by a Harris corner detector and stereo-triangulation [5]. The transformation from the phantom to the camera ($^{C}T_{Ph}$) is solved in the same way except the points are the four centers of the NDI markers and their locations in the camera images are selected manually.

$$\begin{bmatrix} a \\ b \\ c \\ 1 \end{bmatrix}^{C} = {}^{C}T_{T}\,{}^{T}T_{I} \begin{bmatrix} x \\ y \\ 0 \\ 1 \end{bmatrix}^{I} \tag{1}$$

For each LUS image of the N-wire phantom, the location in the phantom coordinate system where the wires intersect the ultrasound imaging plane (d,e,f) are calculated by segmenting the wire ultrasound points and using the distance between the points and the known geometry of the N-wire phantom. The ultrasound calibration matrix ($^{T}T_{I}$) is solved by using a corresponding point algorithm [5] between the N-wire points (d,e,f), projected from the phantom to LUS transducer marker coordinate system, (see equation (2)) and the same N-wire points (x,y) in the ultrasound image coordinate system. Ultrasound segmentation is done via a semi-automatic algorithm which finds the location of each wire by finding the centroid of the ultrasound image pixels associated with each wire.

$${}^{T}T_{C}\,{}^{C}T_{Ph} \begin{bmatrix} d \\ e \\ f \\ 1 \end{bmatrix}^{Ph} = {}^{T}T_{I} \begin{bmatrix} x \\ y \\ 0 \\ 1 \end{bmatrix}^{I} \tag{2}$$

In total, 30 LUS transducer poses were captured for calibration. The 30 poses were randomly assigned to ten groups of 10, ten groups of 15 and one group of 30 and the ultrasound calibration matrix for each group was calculated. During ultrasound calibration, the LUS transducer covered an approximately uniform range within a 5×5×20 mm cuboid and Euler angles of 23°, 11°, and 23° about the x, y and z axes of the LUS transducer marker coordinate system of the first LUS transducer pose [Figure 1].

In summary we built our experimental apparatus so we could compare the combination of a wide baseline camera for ultrasound calibration and a narrow baseline camera for tracking to the combination of a narrow baseline camera for both ultrasound calibration and tracking.

2.2 Experiments

2.2.1 Point Reconstruction Accuracy and Precision

To estimate the pinhead's location in the camera coordinate system, it is segmented from each ultrasound image and its location is transformed to the camera coordinate system as shown in equation (1). Its actual location is determined by stereo triangulation of the pinhead location after draining the fluid medium. Accuracy is the Euclidean distance from the average of the estimated pinheads location to the actual pinhead location. Precision is the average Euclidean distance from each estimated pinhead location point to the centroid of those points. These measures account for errors in calibration as well as alignment, segmentation, tracking and other errors [6]. However, we kept alignment, segmentation and tracking constant across experiments so the changes in accuracy and precision are primarily due to the different ultrasound calibration matrices. The same 22 LUS transducer poses were used for all point reconstruction experiments. The LUS transducer covered an approximately uniform range within a 6×8×10 mm cuboid and Euler angles ranged over 22°, 16°, and 28° about the x, y and z axes respectively of the LUS transducer marker coordinate system of the first LUS transducer pose. The pinhead is plastic and has a diameter of 2.5 mm.

2.2.2 Point Reconstruction Accuracy as a Function of Focal Length

In this experiment the change in accuracy and precision is calculated for a change of focal length from 100 mm to 160 mm. The focal length of the stereo laparoscope was changed to 160 mm, the LUS transducer was moved to a distance of about 160 mm from the stereo laparoscope and 16 new LUS transducer poses were captured. The location of the LUS transducer was calculated using the 100 mm focal length camera calibration parameters and separately with the 160 mm focal length camera calibration parameters. Both sets of camera calibration parameters were calculated with 20 images of an 8 × 10 checkerboard and the Caltech Camera Calibration toolbox [2]. The stereo laparoscope is set to a focal length of 100 mm or 160 mm by placing a checkerboard perpendicular to the viewing direction at those respective distances and adjusting the focus until

the checkerboard is sharply in focus. This approach is necessary because the da Vinci application programming interface does not report the focal length.

3 Results

3.1 Point Reconstruction Accuracy and Precision

The wide baseline approach for calibration improved accuracy (reduced point target localization error) from 3.1 mm to 1.3 mm when 30 LUS transducer poses were used for calibration (Table 1). A similar trend was seen for 10 and 15 calibration poses. A greater number of poses appear to help repeatability of the calibration.

Table 1. Point reconstruction accuracy (mm) ± standard deviation for the combination of narrow baseline calibration and tracking and the combination of wide baseline calibration and narrow baseline tracking. 30 LUS transducer poses were captured for calibration and randomly assigned to ten groups of 10, ten groups of 15 and one group of all 30 poses.

Stereo camera type for ultrasound calibration	Stereo camera type for tracking LUS	# of calibration poses		
		10	15	30
Narrow baseline	Narrow baseline	3.3 ± 1.3	3.3 ± 0.9	3.1
Wide baseline	Narrow baseline	1.5 ± 0.4	1.4 ± 0.3	1.3

The wide baseline approach for calibration improved precision a small amount (Table 2).

Table 2. Point reconstruction precision (mm) ± standard deviation for the combination of narrow baseline calibration and tracking and the combination of wide baseline calibration and narrow baseline tracking. 30 LUS transducer poses were captured for calibration and randomly assigned to ten groups of 10, ten groups of 15 and one group of all 30 poses.

Stereo camera type for ultrasound calibration	Stereo camera type for tracking LUS	# of calibration poses		
		10	15	30
Narrow baseline	Narrow baseline	1.3 ± 0.2	1.4 ± 0.1	1.3
Wide baseline	Narrow baseline	1.2 ± 0.1	1.1 ± 0.1	1.2

3.2 Point Reconstruction Accuracy as a Function of Focal Length

Table 3 shows the accuracy and precision of the point reconstruction test after moving the LUS transducer from a distance of 100 mm to 160 mm and changing the focal length from a distance of 100 mm to 160 mm without updating the camera calibration parameters. The change of focal length without updating the camera calibration parameters decreases accuracy (increased point target localization error) to about 20 mm. When the stereo camera is calibrated at 160 mm

Table 3. Point reconstruction results (mm) ± std for the LUS transducer at a distance of 160 mm from the narrow baseline camera. The focal length (mm) is the focal length at which the stereo camera calibration parameters were calculated. 30 LUS transducer poses were captured for calibration and randomly assigned to ten groups of 15.

Stereo camera type for ultrasound calibration	Stereo camera type for tracking LUS	Focal Length (mm)	Accuracy (mm)	Precision (mm)
Narrow baseline	Narrow baseline	100	19.2 ± 0.7	1.8 ± 0.2
Wide baseline	Narrow baseline	100	20.2 ± 0.2	1.5 ± 0.1
Narrow baseline	Narrow baseline	160	2.6 ± 1.0	1.8 ± 0.2
Wide baseline	Narrow baseline	160	0.8 ± 0.4	1.5 ± 0.1

and those camera calibration parameters are used accuracy returns to 0.8 mm and 2.6 mm for wide baseline and low baseline camera tracking respectively. These results are similar to what was observed when the LUS transducer was at a distance of 100 mm.

4 Discussion and Conclusion

We have shown a millimeter level of accuracy for an augmented reality LUS system via direct visual tracking using a stereo laparoscope, suggesting it is a viable option for guidance in minimally invasive surgery. When we implement our proposed method of using a wide baseline (75 mm) stereo camera for ultrasound calibration and a narrow baseline (5 mm) stereo laparoscope for tracking the accuracy is 1.3 mm (Table 1). When the narrow baseline camera system is used for ultrasound calibration and tracking, accuracy of 3.1 mm is achieved. This reinforces the need for careful consideration of the ultrasound calibration step.

Most other research groups that developed augmented reality LUS systems used tracking systems that include an external base coordinate system such as optical tracking [9], electromagnetic tracking [3], and a combination of optical tracking and electromagnetic tracking [4]. These groups have reported point reconstruction errors in the approximate range of 1.5 mm and 3 mm. It should be noted that direct comparisons of accuracy results are difficult because of differences in apparatus, tests and definitions of accuracy. The novelty in our work is the use of a different stereo camera system for the ultrasound calibration and the direct visual tracking of the LUS transducer with a stereo laparoscope. The concept of using a different sensor for ultrasound calibration is broadly applicable. With the increasing adoption of the da Vinci, Viking and Olympus stereo laparoscopes, the need for understanding the challenges associated with direct visual tracking with a stereo laparoscope will continue to grow. Furthermore, direct visual tracking has an elegant simplicity that minimizes the extra equipment required to implement the system and electromagnetic field distortion is not a concern. One drawback is the need for a line of sight between the laparoscope and the LUS transducer, but this is naturally performed by the surgeon when placing the LUS transducer over a region of interest. A second drawback is that

blood or other fluid may obscure part of the LUS checkerboard optical markers. However, as long as part of the checkerboard remains visible the LUS transducer can still be tracked, albeit with reduced accuracy.

To further understand the effect of camera baseline on accuracy we calculated the accuracy of the combination of wide baseline calibration and tracking and the accuracy of the combination of narrow baseline calibration with wide baseline tracking. The results were 0.6 mm and 2.45 mm respectively. For these experiments we used the same 30 LUS transducer poses that were captured for calibration and the same 22 LUS transducer poses that were captured to determine the accuracy and precision. Thus, the best case accuracy is 0.6 mm and we surmise that using a narrow baseline camera for tracking decreases accuracy (increases point target localization error) by about 0.7 mm to the overall accuracy of 1.3 mm (see Table 1).

The next steps for this project include real-time implementation, clinical validation and further accuracy improvements. The custom-built pick-up LUS [15] used in this experiment has a built-in EM sensor so visual tracking and EM sensor fusion is possible [4]. Further work will also address our finding that the change in stereo laparoscope camera focal length during the operation has a dramatic effect on the error of the point reconstruction accuracy. In future work we plan to match the camera calibration parameters to a range of pre-calibrated setting by using the checkerboard that is already mounted on the LUS transducer as a guide to the approximate camera calibration parameters. Several applications we may pursue for the stereo laparoscope augmented reality LUS system are guidance during MIS hepatic or renal tumour resections, pre-operative CT scan to intra-operative ultrasound registration and display of absolute elastography images [14]. Regardless, the stereo laparoscope augmented reality LUS system is broadly applicable across a large range of surgeries.

Acknowledgements. This work is supported by CIHR, NSERC and the Institute for Computing, Information and Cognitive Systems (ICICS) at UBC. The semi-automatic ultrasound segmentation and N-wire ultrasound calibration MATLAB code and GUI were written by Jeff Abeysekera at the University of British Columbia.

References

1. Ali, A., Logeswaran, R.: A visual probe localization and calibration system for cost-effective computer-aided 3d ultrasound. Computers in Biology and Medicine 37(8), 1141–1147 (2007)
2. Bouget, J.Y.: Camera calibration toolbox for matlab @ONLINE (2013), `http://www.vision.caltech.edu/bouguetj/calib_doc/index.html`
3. Cheung, C.L., Wedlake, C., Moore, J., Pautler, S.E., Peters, T.M.: Fused video and ultrasound images for minimally invasive partial nephrectomy: A phantom study. In: Jiang, T., Navab, N., Pluim, J.P.W., Viergever, M.A. (eds.) MICCAI 2010, Part III. LNCS, vol. 6363, pp. 408–415. Springer, Heidelberg (2010)

4. Feuerstein, M., Reichl, T., Vogel, J., Traub, J., Navab, N.: Magneto-optical tracking of flexible laparoscopic ultrasound: model-based online detection and correction of magnetic tracking errors. IEEE Transactions on Medical Imaging 28(6), 951–967 (2009)
5. Horn, B.K.: Closed-form solution of absolute orientation using unit quaternions. JOSA A 4(4), 629–642 (1987)
6. Hsu, P.W., Treece, G.M., Prager, R.W., Houghton, N.E., Gee, A.H.: Comparison of freehand 3-d ultrasound calibration techniques using a stylus. Ultrasound in Medicine & Biology 34(10), 1610–1621 (2008)
7. Hubens, G., Coveliers, H., Balliu, L., Ruppert, M., Vaneerdeweg, W.: A performance study comparing manual and robotically assisted laparoscopic surgery using the da Vinci system. Surgical Endoscopy 17(10), 1595–1599 (2003)
8. Langø, T., Vijayan, S., Rethy, A., Våpenstad, C., Solberg, O.V., Mårvik, R., Johnsen, G., Hernes, T.N.: Navigated laparoscopic ultrasound in abdominal soft tissue surgery: technological overview and perspectives. International Journal of Computer Assisted Radiology and Surgery 7(4), 585–599 (2012)
9. Leven, J., et al.: DaVinci canvas: A telerobotic surgical system with integrated, robot-assisted, laparoscopic ultrasound capability. In: Duncan, J.S., Gerig, G. (eds.) MICCAI 2005. LNCS, vol. 3749, pp. 811–818. Springer, Heidelberg (2005)
10. Mercier, L., Langø, T., Lindseth, F., Collins, D.L., et al.: A review of calibration techniques for freehand 3-d ultrasound systems. Ultrasound in Medicine and Biology 31(2), 143–166 (2005)
11. Oates, C.: Towards an ideal blood analogue for doppler ultrasound phantoms. Physics in Medicine and Biology 36(11), 1433 (1991)
12. Pratt, P., Di Marco, A., Payne, C., Darzi, A., Yang, G.-Z.: Intraoperative ultrasound guidance for transanal endoscopic microsurgery. In: Ayache, N., Delingette, H., Golland, P., Mori, K. (eds.) MICCAI 2012, Part I. LNCS, vol. 7510, pp. 463–470. Springer, Heidelberg (2012)
13. Schneider, C.M., Dachs II, G.W., Hasser, C.J., Choti, M.A., DiMaio, S.P., Taylor, R.H.: Robot-assisted laparoscopic ultrasound. In: Navab, N., Jannin, P. (eds.) IPCAI 2010. LNCS, vol. 6135, pp. 67–80. Springer, Heidelberg (2010)
14. Schneider, C., Baghani, A., Rohling, R., Salcudean, S.: Remote ultrasound palpation for robotic interventions using absolute elastography. In: Ayache, N., Delingette, H., Golland, P., Mori, K. (eds.) MICCAI 2012, Part I. LNCS, vol. 7510, pp. 42–49. Springer, Heidelberg (2012)
15. Schneider, C., Guerrero, J., Nguan, C., Rohling, R., Salcudean, S.: Intra-operative "Pick-up" ultrasound for robot assisted surgery with vessel extraction and registration: A feasibility study. In: Taylor, R.H., Yang, G.-Z. (eds.) IPCAI 2011. LNCS, vol. 6689, pp. 122–132. Springer, Heidelberg (2011)
16. Stoyanov, D., Darzi, A., Yang, G.Z.: Laparoscope self-calibration for robotic assisted minimally invasive surgery. In: Duncan, J.S., Gerig, G. (eds.) MICCAI 2005. LNCS, vol. 3750, pp. 114–121. Springer, Heidelberg (2005)
17. Våpenstad, C., Rethy, A., Langø, T., Selbekk, T., Ystgaard, B., Hernes, T.A.N., Mårvik, R.: Laparoscopic ultrasound: a survey of its current and future use, requirements, and integration with navigation technology. Surgical Endoscopy 24(12), 2944–2953 (2010)
18. Wang, D., Bello, F., Darzi, A.: Augmented reality provision in robotically assisted minimally invasive surgery. International Congress Series, vol. 1268, pp. 527–532. Elsevier (2004)